

Attenuation of ultraviolet irradiance in North European coastal waters*

OCEANOLOGIA, 43 (2), 2001.
pp. 139–168.

© 2001, by Institute of
Oceanology PAS.

KEYWORDS

UV irradiance
Attenuation
Coastal waters
Fjords
Straits
Optical properties

EYVIND AAS
Department of Geophysics,
University of Oslo,
POB 1022 Blindern, N-0315 Oslo, Norway;
e-mail: eyvind.aas@geofysikk.uio.no

NIELS K. HØJERSLEV
Niels Bohr Institute of Astronomy,
Physics and Geophysics,
University of Copenhagen,
Juliane Maries Vej 30, DK-2100 Copenhagen Ø, Denmark;
e-mail: nkh@gfy.ku.dk

Manuscript received 20 April 2001, accepted 27 April 2001.

Abstract

A total of 439 measurements of downward ultraviolet irradiance in North European coastal waters have been analysed, half of which have been taken from other authors. The depths $Z(10\%)$ where the irradiance is reduced to 10% of its

* The Norwegian Research Council supported the field work in the Norwegian Coastal Current during 1967–71 through the International Biological Program, and in the Oslo Fjord in 1973 by a separate project. Measurements in the Hardanger Fjord in 1967 were supported by A/S Norsk Varekrigsforsikrings Fond, and in 1970 by the Nordic Collegium for Physical Oceanography.

The measurements in the Kattegat, the Skagerrak, the German Bight, and the Hardanger Fjord in 1972 were supported by the Danish Space Agency, the Danish Ministry of the Environment, the Danish Council for the Natural Sciences, the Nordic Collegium for Physical Oceanography, and the University of Bergen.

surface value vary by one order of magnitude in the open coastal waters, both at wavelengths of 310 nm (0.3–10.4 m) and 380 nm (1.2–13.0 m). In the fjords and estuaries the depth ranges are reduced to 0.08–6.1 m at 310 nm and 0.18–7.7 m at 380 nm. Mixing with saline ocean waters can increase these light penetration depths to more than 10 m, while river water can reduce them to a few centimetres.

1. Introduction

The energy of the daylight spectrum and seawater transmittance both decrease steeply from 450 nm towards shorter wavelengths. As a result a marine irradiance meter for the spectral region 280–315 nm (ultraviolet B) or 315–400 nm (ultraviolet A) requires a very high sensitivity compared to an instrument intended for the visible part of the spectrum (400–750 nm). During the early years of optical oceanography, irradiance measurements in the ultraviolet (UV) part of the spectrum were inhibited by the lack of proper sensors. The ordinary irradiance meters usually consisted of an opal glass acting as a cosine or Lambert collector, a glass window, some glass or interference filters, and either a photo-electric cell (introduced in the twenties and thirties) or a photomultiplier tube (available from the fifties). The resulting spectral sensitivity permitted irradiance measurements to be made for wavelengths down to about 360 nm within the upper layers of the sea. Jerlov substituted the opal glass and the glass window with three hemispheres of quartz filled with special chemical solutions, thus obtaining a detector with its peak sensitivity at about 310 nm (Johnson 1946). During the seventies photomultipliers with enhanced sensitivity in the UVB part of the spectrum became available, and later on improved silicon photodiodes enabled the construction of special instruments for recording irradiance at wavelengths down to and below 300 nm.

The UV region is important for several reasons; it represents the short-wave side of the spectrum of solar radiant energy, and the UV radiation reaching the surface of the ocean, although low in energy, can produce positive as well as very negative biological effects. The ability of the short-wave radiation to activate the production of vitamin D, to produce erythema and to damage DNA molecules is well known. Cod-liver oil is one of the main sources of vitamin D, although the cod itself is usually found at depths where there is practically no UV radiation left. Atkins & Poole (1933) suggested that the copepods, which are the chief source of food for the fish and which in the English Channel were found mainly at a ‘moderate depth’, could be the source of the vitamin D. Their attempted recordings of UV irradiance were made to see if there was sufficient anti-rachitic radiation at the different depths to support this hypothesis. The first UVB measurements made by Jerlov in 1944–45 (when he still bore the name of Johnson) were similarly related to the study of the marine production of

vitamin D (Johnson 1946). The comprehensive monograph entitled ‘The Role of Solar Ultraviolet Radiation in Marine Ecosystems’ (Calkins 1982) summed up the physical and biological aspects of marine UV radiation that were known by the beginning of the eighties.

The discovery of ozone depletion over Antarctica in 1980–84 (Farman et al. 1985, Farman & Gardiner 1987) and the similar discovery in the Arctic a decade later (Fahey 1995) drew new attention to the harmful effects of UVB irradiance, and numerous investigations of marine UV irradiance were initiated (e.g. Gieskes & Kraay 1990, Smith et al. 1992, Helbling et al. 1994, Piazena & Häder 1994, Montecino & Pizarro 1995, Aas & Høkedal 1996, Stambler et al. 1997, Bischof et al. 1998, Kuhn et al. 1999, Kjeldstad et al. 2000, Hanelt et al. 2001).

North European oceanic and coastal waters contain important spawning and fishing grounds where increased UV irradiance may lead to damaging biological effects. Already in 1967, as a part of the International Biological Program, marine biologists in Norway started a field investigation in the Norwegian Coastal Current, where the possible harmful influence of UV radiation on the eggs and larvae of cod and herring was one of the issues. The biological part of the project came up against unexpected problems, but the irradiance measurements, obtained with old-fashioned equipment, even today represent the only description of the UVA transparency in this current (Aas 1969, Aas et al. 2001).

It must be said that the mapping of UV attenuation in North European seawaters is rather incomplete. A review of our present knowledge of the Arctic oceanic areas has been made by Aas et al. (2001). UV transparency in Nordic coastal waters and fjords have already been described by the present authors (Aas 1969, 1971, Højerslev 1973, 1974, 1978, 1982, Højerslev & Lundgren 1977, Højerslev & Aas 1991, Aas & Høkedal 1996, Aas et al. 2001), but more details and new results will be presented here. The emphasis will be on these investigations, but a comparison will also be made with the results of other authors (Johnson 1946, Johnson & Kullenberg 1946, Aarthun 1958, Calkins & Thordardottir 1982, Piazena & Häder 1994, Aarseth 1997, Bischof et al. 1998, Kjeldstad et al. 2000, Hanelt et al. 2001). The aim of this paper is to sum up what we know today about UV attenuation in North European coastal waters in order to provide a basis for future investigations.

2. Material and methods

2.1. Field observations

In this paper we define coastal water either as water no farther than 100 km from a coast, or as water that clearly differs from adjacent oceanic

water masses in its hydrographical and optical properties. Stations within 100 km of the Icelandic coast have been included, but not stations within a similar distance of the Faroes, since the water type at the latter stations is clearly oceanic. At Svalbard we have included the fjords but not the stations along the coast.

Measurements of UVB irradiance were made at 126 stations in Danish coastal waters, mainly in the German Bight (1979, 1981), the Kattegat (1979) and the Eastern Skagerrak (1979). Data of UVA irradiance was obtained at 14 stations in Baltic (1973) and Danish (1976–77) coastal waters. In the eutrophic Oslo Fjord UVA irradiance was recorded at 24 stations (1967, 1973) and UVB irradiance at 5 stations (2000), whereas 13 stations yielding observations of UVA irradiance were obtained in the glacier-fed Hardanger Fjord (1967, 1970, 1972). North of 62°N, in the Norwegian Coastal Current, measurements of UVA irradiance were made at 14 stations (1967–71) and west of Iceland at two stations (1973).

2.2. Instruments

Downward UVB irradiance was measured by three different single-channel instruments. The Jerlov construction used a selenium photovoltaic cell equipped with a UG5 glass filter and three external hemispheres of quartz filled with solutions of nickel sulphate and picric acid (Johnson 1946, Jerlov 1976, Højerslev 1978). This sensor reached peak sensitivity at 310 nm and had a bandwidth of 15 nm at half peak value. The instrument was used for taking the measurements in the Great Belt (1976) and the German Bight (1979).

The other UVB instruments, constructed by N.K. Højerslev and H. Hundahl, were based on photomultipliers with interference filters; their peak sensitivities lay at 309 and 306 nm, and the corresponding bandwidths were about 5 and 10 nm. The signals were amplified logarithmically, with a resulting sensitivity range of 9–10 decades. Other instrumental details have been presented by Høkedal & Aas (1994). The first of these instruments was applied in the Baltic and the Sound (1977), the Kattegat and the Skagerrak (1979), and the German Bight (1981), and the second instrument was used in the Oslo Fjord (2000).

UVA irradiance was recorded in the Oslo Fjord, the Hardanger Fjord (1967, 1970) and the Norwegian Coastal Current with an instrument consisting of a selenium cell equipped with an opal glass and a UG1 + BG12 broadband filter. The bandwidth of the instrument with filter is about 40 nm. The peak contribution to the signal originates at a wavelength of 380 nm when the instrument is close to the surface, but shifts towards longer

wavelengths with increasing depth. Our analysis has shown, however, that the depths for 10% and 1% of the surface value for irradiance at 380 nm practically coincide with the depths for the corresponding percentages of the instrument signal with this filter. Similarly, the vertical attenuation of downward irradiance at 465 nm could be found from measurements taken with a BG12 + GG5 filter (Jerlov 1951).

Other recordings of UVA irradiance in the Hardanger Fjord (1972), in the Baltic Sea from west of Bornholm to north of Gotland (1973), and west of Iceland (1973) were obtained with an instrument incorporating a photomultiplier and an interference filter at 372 nm (Højerslev 1973, 1974, Højerslev & Lundgren 1977). Recordings of irradiance at 375 nm in Danish coastal waters (1976–77) were made with an instrument provided with a Zeiss double-monochromator. For the sake of simplicity, all UVB results presented in this paper have been assigned to 310 nm and all UVA results to 380 nm, by assuming that the actual differences in wavelength are negligible compared to other errors.

2.3. Presentation of observations

The UV attenuation may be expressed by different quantities, and the best way to present conditions at a single station may be by the vertical profile of downward irradiance E_d , as in Fig. 1. For a large number of stations, however, this way of presenting the attenuation becomes impractical, and a better method may be to apply the slope of the vertical

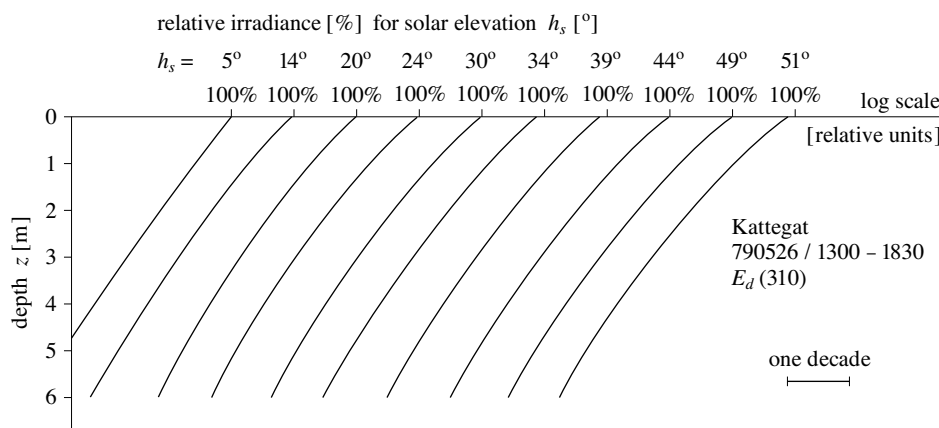


Fig. 1. Vertical profiles of downward irradiance $E_d(310)$ in the Kattegat for different solar elevations h_s

profile, quantified by the vertical attenuation coefficient K_d . It is defined for a certain depth z by

$$K_d(z) = -\frac{1}{E_d(z)} \frac{dE_d(z)}{dz}, \quad (1)$$

where z is the vertical co-ordinate, positive downwards, or it can be defined as the average value for a depth interval z_1 – z_2 by

$$K_d = \frac{-1}{z_2 - z_1} \ln \frac{E_d(z_2)}{E_d(z_1)}. \quad (2)$$

This coefficient has the useful quality that it is an approximate linear function of the concentration of light-absorbing matter. An expression for K_d , based on the Gershun equation (Gershun 1939) and eq. (1), is (Aas 1976, Aas et al. 2001)

$$K_d \approx \frac{a}{\mu_d} (1 + 3R), \quad (3)$$

where a is the absorption coefficient, μ_d is the average cosine of the downward radiance, and R is the ratio between the upward and downward irradiances. The absorption coefficient consists of four main components: (1) pure seawater, (2) phytoplankton and associated debris, (3) inorganic particles, and (4) yellow substance. In the open ocean the variation of K_d is dominated by the contribution of (2), while in coastal waters (3) and (4) may be of a similar importance. The spectral properties of these components have been discussed by Aas et al. (2001).

Our measurements have shown that R is usually $< 1\%$ for UV irradiance in North European coastal waters, implying that K_d/a varies as $1/\mu_d$ according to eq. (3). (The observed value of R in the Kattegat in May 1979 was 0.04%, while in the northern Barents Sea in August 1991 it was 0.06–0.08% (Høkedal pers. comm.)). In the UV part of the spectrum μ_d will be dominated by the contribution from diffuse sky radiance, resulting in a μ_d beneath the surface of the sea that varies in the narrow range 0.80 ± 0.05 (Aas & Høkedal 1999, Aas et al. 2001). This again means that the influence of solar elevation on the value and variation of K_d is practically negligible.

However, when the slope varies with depth as in Fig. 1, K_d will not have a unique value, but will depend on the type of definition and the depth or depth interval that have been applied. In addition, the physical implications of its numerical value are not always readily seen. We have therefore chosen to represent the UV transparency of the sea water by the quantity $Z(10\%)$, which is the depth at which the surface irradiance is reduced to 10% of its surface value; the surface value is defined as being equal to 100% just beneath the surface. According to eq. (2) the relation between the light penetration depth $Z(10\%)$ and K_d is

$$Z(10\%) = -\ln(0.10)/K_d = 2.30/K_d, \quad (4)$$

where K_d is the mean value of the vertical attenuation coefficient between the surface and depth $Z(10\%)$.

The quantity $Z(10\%)$ is a uniquely defined and useful optical quantity for characterising seawaters and is well suited to illustrate the spatial variation of the water transparency. For cases where K_d is constant with depth, the quantity $Z(1\%)$, which is the depth where the irradiance is reduced to 1% of its surface value, is exactly twice the value of $Z(10\%)$. In layered surface waters $Z(1\%)$ often becomes greater, as will be shown below.

2.4. Calculated values of K_d

No recordings of UVB irradiance in the Norwegian Coastal Current have been published, but several recordings at 380 and 465 nm were made during the International Biological Program in 1967–69, and a few recordings were added in 1971. A simple two-component model, by which $K_d(310)$ can be predicted from measured values of $K_d(380)$ and $K_d(465)$, was tentatively constructed for these waters by Aas et al. (2001). Estimates of $K_d(310)$ and $K_d(380)$ can also be produced from $K_d(410)$ and $K_d(465)$.

The model is based on the assumption that the Norwegian Coastal Current north of 62°N is strongly influenced by the adjacent Atlantic waters. By Atlantic waters are meant waters originating mainly from the Norwegian Current, characterised by salinities on the Practical Salinity Scale close to or above 35.0 and very low contents of yellow substance. Optically, Atlantic waters behave as if they had only one optical variable, namely the particle content. Hence it is assumed that the vertical attenuation coefficient $K_A(\lambda)$ of downward irradiance at the wavelength λ in these waters can be separated into a constant term $K_w(\lambda)$ and a variable term $K_p(\lambda)$ due to the particle content:

$$K_A(\lambda) = K_w(\lambda) + K_p(\lambda). \quad (5)$$

K_d (or K_A) is not an inherent optical property since it depends on the apparent properties μ_d and R according to eq. (3), but the separation in eq. (5) can still be justified, provided μ_d is almost constant and R is $\ll 1$ or almost constant. The term $K_p(\lambda)$ can be related to $K_p(465)$ by a function $B(\lambda)$ so that $K_p(\lambda) = B(\lambda) K_p(465)$, and eq. (5) may be written

$$K_A(\lambda) = K_w(\lambda) + B(\lambda) K_p(465). \quad (6)$$

At 465 nm this equation becomes

$$K_A(465) = K_w(465) + K_p(465). \quad (7)$$

By eliminating $K_p(465)$ between eqs. (6) and (7) we obtain

$$K_A(\lambda) = [K_w(\lambda) - B(\lambda) K_w(465)] + B(\lambda) K_A(465), \quad (8)$$

which describes a linear relation between the observed coefficients $K_A(\lambda)$ and $K_A(465)$. Equations of type (8) above formed the basis for Jerlov's classification of oceanic and coastal waters (e.g. Jerlov 1976), and they have been validated by Austin & Petzold (1984, 1990). We have found, however, that the constants of eq. (8) may change from one oceanic area to another. For the Atlantic waters of the Norwegian Sea the relation at 310 and 465 nm has been observed to be (Højerslev & Aas 1991)

$$K_A(310) = 0.078 \text{ m}^{-1} + 1.04 K_A(465); \quad r = 0.998, \quad (9)$$

where r is the coefficient of correlation, and similarly, the relation for 380 and 465 nm has been observed as (Aas et al. 2001)

$$K_A(380) = 0.040 \text{ m}^{-1} + 1.01 K_A(465); \quad r = 0.997. \quad (10)$$

It is crucial that these equations appear to be valid only for the type of water from which they were obtained, i.e. yellow substance-poor North Atlantic waters.

The model for the Norwegian Coastal Current assumes that the vertical attenuation coefficient $K_d(\lambda)$ at wavelength λ can be divided into an Atlantic part $K_A(\lambda)$ that follows eqs. (9)–(10), and an added part $K_y(\lambda)$ due to the higher content of yellow substance, so that

$$K_d(\lambda) = K_A(\lambda) + K_y(\lambda). \quad (11)$$

In this model it is further assumed that the spectral variation of $K_y(\lambda)$ can be expressed by an exponential function similar to the spectral variation of the absorption coefficient of yellow substance,

$$K_y(\lambda) \approx K_y(465)e^{\gamma(465-\lambda)}, \quad (12)$$

where γ is in units of nm^{-1} and λ is in nm. When λ is known and the downward irradiance has been measured at 380 and 465 nm, $K_d(310)$ becomes a function of the observed coefficients $K_{\text{obs}}(380)$ and $K_{\text{obs}}(465)$. The mean value of γ in the northern part of the Norwegian Coastal Current has been observed to be 0.020 nm^{-1} (Aas et al. 2001), and by inserting this value in eq. (12), eq. (11) produces

$$K_d(310) \approx K_A(310) + 22.2 K_y(465), \quad (13)$$

$$K_{\text{obs}}(380) \approx K_A(380) + 5.47 K_y(465), \quad (14)$$

$$K_{\text{obs}}(465) = K_A(465) + K_y(465). \quad (15)$$

By combining eqs. (9)–(10) and (13)–(15) it now becomes easy to deduce that

$$K_d(310) = -0.112 \text{ m}^{-1} + 4.74 K_{\text{obs}}(380) - 3.75 K_{\text{obs}}(465). \quad (16)$$

An empirical relation for the Atlantic waters of the Greenland Sea, presented by Aas et al. (2001), is

$$K_A(410) = 0.029 \text{ m}^{-1} + 0.92 K_A(465); \quad r = 0.989. \quad (17)$$

The same procedure as above now gives

$$K_d(310) = -0.216 \text{ m}^{-1} + 10.15 K_{\text{obs}}(410) - 8.30 K_{\text{obs}}(465), \quad (18)$$

$$K_d(380) = -0.035 \text{ m}^{-1} + 2.14 K_{\text{obs}}(410) - 0.916 K_{\text{obs}}(465). \quad (19)$$

The quasi-empirical relationships of eqs. (16) and (18)–(19) have not been validated directly, but several independent investigations indicate that the model works satisfactorily in yellow substance-rich waters. To see this we have to deduce an expression for K_d as a continuous function of λ in the range 310–465 nm. We start by combining eqs. (5) and (11)

$$K_d(\lambda) - K_w(\lambda) = K_p(\lambda) + K_y(\lambda). \quad (20)$$

The linear slopes of eqs. (9), (10) and (17) are close to 1, proving that the spectral dependence of K_p is small. We may use this fact to approximate $B(\lambda)$ of eq. (6) by an exponential function

$$K_p(\lambda) = K_p(465)B(\lambda) = K_p(465)e^{p\Delta\lambda}, \quad (21)$$

where $p \approx 0.00012 \text{ nm}^{-1}$ is the empirical semilogarithmic spectral slope of $B(\lambda)$ or $K_p(\lambda)$ and $\Delta\lambda = (465 \text{ nm} - \lambda)$. The exponential function describes the observed values of $B(\lambda)$ (Aas et al. 2001) with an average relative error of 6%.

Both K_p (eq. (21)) and K_y (eq. (12)) are now expressed as exponential functions of $p\Delta\lambda$ and $\gamma\Delta\lambda$ respectively. If these exponential functions are expanded in series, eq. (20) becomes

$$\begin{aligned} K_d(\lambda) - K_w(\lambda) &= K_p(465)[1 + p\Delta\lambda + \dots] + K_y(465)[1 + \gamma\Delta\lambda + \dots] \\ &= [K_p(465) + K_y(465)] \left[1 + \frac{K_p(465)p + K_y(465)\gamma}{K_p(465) + K_y(465)} \Delta\lambda + \dots \right]. \end{aligned} \quad (22)$$

By introducing

$$K_0(465) = K_p(465) + K_y(465) \quad (23)$$

and

$$s = \frac{K_p(465)p + K_y(465)\gamma}{K_p(465) + K_y(465)} \quad (24)$$

eq. (22) may be written

$$K_d(\lambda) - K_w(\lambda) = K_0(465)[1 + s\Delta\lambda + \dots]. \quad (25)$$

The right-hand side of this equation resembles a serial expansion of the exponential function $K_0(465) \exp(s\Delta\lambda)$. The expansion is correct to the first order, but differences occur in the second and higher order terms. However, all the differences involve products with the slope p , and since $p \ll 1$, the errors become small. Consequently, the serial expansion indicated in eq. (25) may be approximated by

$$K_d(\lambda) - K_w(\lambda) \approx K_0(465)e^{s\Delta\lambda}. \quad (26)$$

When $K_w(\lambda) \ll K_d(\lambda)$ this relation can be written

$$K_d(\lambda) \approx K_0(465)e^{s\Delta\lambda}. \quad (27)$$

The slope s is the weighted average between the values of p and γ , corresponding to the range 0.00012–0.020 nm⁻¹ for the Norwegian Coastal Current. A recent discussion of the spectral slope γ of yellow substance has been given by Høgerslev & Aas (2001).

Morris et al. (1995) found for a large selection of lakes that K_d was best estimated throughout the UVA and UVB region by an expression similar to eq. (27) with $s = 0.01347$ nm⁻¹. Laurion et al. (1997) obtained an accurate description of $K_d(\lambda)$ in sub-arctic lakes for the range 320–440 nm by eq. (27) with $s = 0.0151$ nm⁻¹. In the Trondheim Fjord Kjeldstad et al. (2000) found that K_d followed an exponential function of the wavelength from 305 to 380 nm. Their spectral slope varied with season from 0.0114 to 0.0157 nm⁻¹. Markager & Vincent (2000) added a constant term to the right-hand side of eq. (27) and obtained a better fit between observations and equation for high-altitude Arctic lakes. Their investigated range was 360–500 nm, and the mean value of s was 0.0174 nm⁻¹. These results imply that if $K_d(310)$ and $K_d(380)$ are known, $K_d(\lambda)$ may be inter- or extrapolated over the whole UVB and UVA range with good accuracy.

3. Hydrography of the investigated areas

The Skagerrak and the Kattegat are parts of the transition zone between the North Sea and the Baltic Sea, and they constitute an area where three primary water types mix: (1) Baltic Sea water of salinity 8.0 and an absorption coefficient $a_y(380)$ of yellow substance equal to 0.96 m⁻¹, (2) North Sea water of Atlantic origin with salinity 35.0 and $a_y(380) = 0.07$ m⁻¹, and (3) water from the German Bight with salinity 31.0 and $a_y(380) = 1.50$ m⁻¹ (Høgerslev et al. 1996). The Baltic Current supplies the Baltic water, and the very variable and often very weak Jutland Current supplies the water from the German Bight. North Sea water does not enter the area as a regular surface current, but its contribution of yellow substance-poor waters of high salinity to the central part and the deeper layers of the Skagerrak is crucial for the hydrographical and optical properties of the region.

The Baltic Current passes through the Belts and the Sound, continues northwards through the Kattegat and the Eastern Skagerrak, and when it reaches the mouth of the Oslo Fjord it is forced towards the south-west and follows the Norwegian coast as the Norwegian Coastal Current. Later the current turns first westwards and then northwards and finally enters the Barents Sea. It transports an average freshwater supply of 15×10^3 m³ s⁻¹

from the Baltic Sea (Wyrтки 1954), and during its course along the Norwegian coast it receives an additional $12 \times 10^3 \text{ m}^3 \text{ s}^{-1}$ of freshwater (Tollan 1976). The total transport of the current has been calculated to be in the range $0.5\text{--}1.0 \times 10^6 \text{ m}^3 \text{ s}^{-1}$ (Furnes & Sælen 1977, Aure & Sætre 1981, Dooley & Furnes 1981). The current may start in the Baltic with the aforementioned typical salinity of 8, but outside the Oslo Fjord it increases to 23 in summer or 29 in winter, and when it enters the Barents Sea the average salinity is about 34 (Midttun 1971).

The Oslo Fjord and the Hardanger Fjord, situated in the south-eastern and western parts of Norway respectively, are interesting because their properties are quite different. The Hardanger Fjord is supplied with freshwater from glaciers and mountainous areas, with a strong maximum river run-off in the summer and a minimum of almost zero during winter. The Oslo Fjord is a typical eutrophic estuary, and the rivers entering the fjord have passed through large agricultural areas and forests; the seasonal variation of the river run-off is less than for the Hardanger Fjord. The freshwater supply to the Inner Oslo Fjord is small, and in this part the range of the surface salinity is typically 18–28, while in the Hardanger Fjord the same range will be 2–34 (Sælen 1967). The optical properties of the latter type of fjord will also show a significant seasonal dependence. In the Sogne Fjord, which is the nearest fjord north of the Hardanger Fjord, the Secchi disc depth has been observed to vary from 1 m in summer (salinity 0.4) to 26 m in winter (salinity 30) (Rustad 1978).

4. Results

Fig. 1 shows the vertical profiles of downward UVB irradiance for different solar elevations at a station in the Kattegat. The spatial distributions of $Z(310, 10\%)$ in the German Bight, the Eastern Skagerrak and the Kattegat are presented in Fig. 2. The values in the figure are averages based on nearby stations. For instance, the 5 values for the German Bight represent 58 stations evenly distributed throughout the area. Figs. 3 and 4 display distributions of $Z(310, 10\%)$ and $Z(380, 10\%)$ within the Norwegian Coastal Current.

The statistical properties of the penetration depths and the corresponding surface salinities are presented in Tables 1 and 2. The results have been ranged according to their mean salinity. The *Baltic-Danish coastal waters* in Table 1 comprise single observations from the Central Baltic [$Z(310, 10\%) = 0.7 \text{ m}$, September 1977], the Great Belt [$Z(310, 10\%) = 0.8 \text{ m}$, August 1976] and the Sound [$Z(310, 10\%) = 2.5 \text{ m}$, November 1977]. In Table 2 *Danish coastal waters* represent the Sound-Kattegat area. The fourteenth station from the *Norwegian Coastal Current*, situated in the harbour of

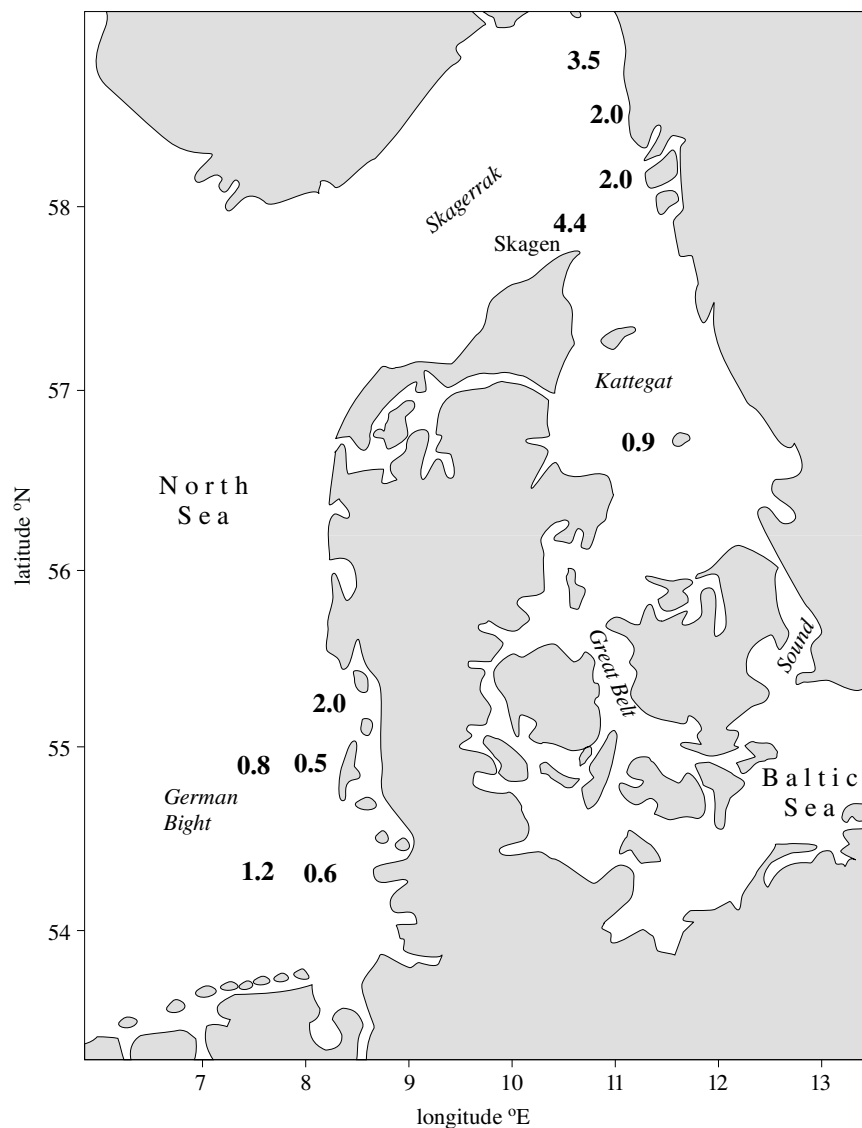


Fig. 2. Distribution of $Z(310, 10\%)$ [m] in the Kattegat (48 stations, May 1979), the Skagerrak (30 stations, March–April 1979) and the German Bight (45 stations, August–September 1979; 13 stations, June 1981). The penetration depths represent the mean values of several closely situated stations

the small fishing village of Hareide, was not included in the statistics of Tables 1–2 because the waters at this location were clearly influenced by local sewage. In the harbour the observed value of $Z(380, 10\%)$ was 4.3 m and the estimated value of $Z(310, 10\%)$ became 1.6 m. The area of the

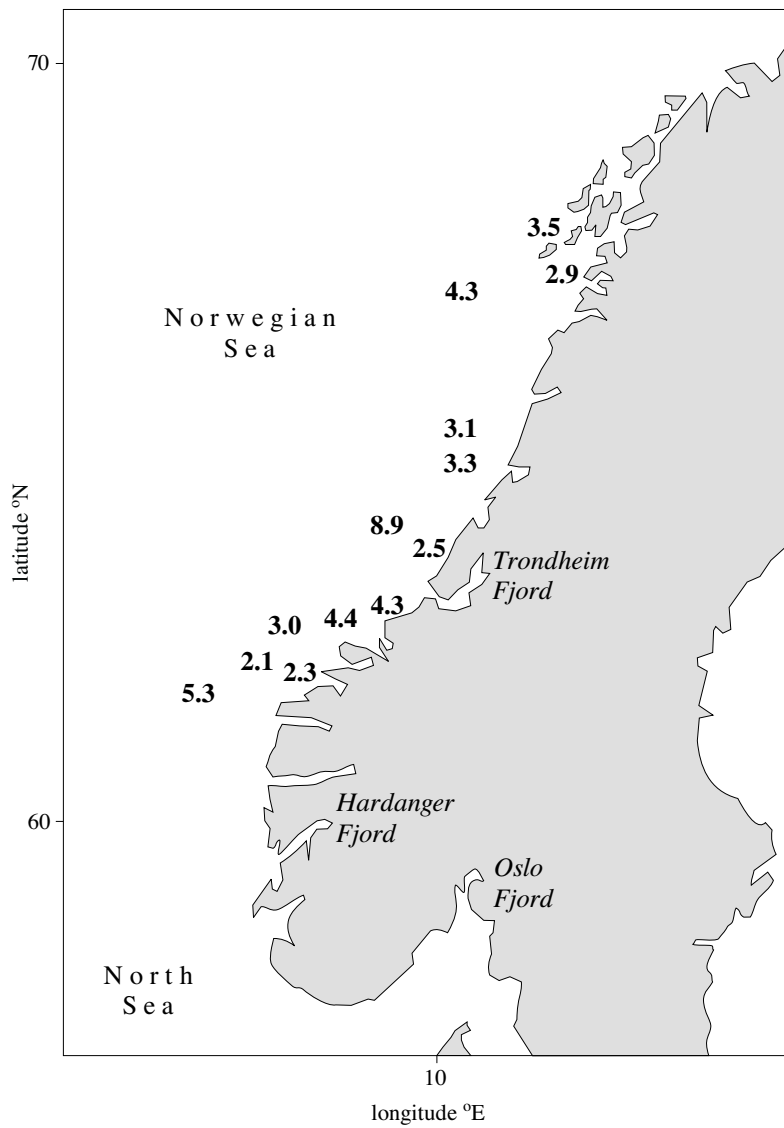


Fig. 3. $Z(310,10\%)$ [m] calculated by eq. (16) for the Norwegian Coastal Current (13 stations)

Inner Oslo Fjord extends from Oslo Harbour 30 km southwards to the city of Drøbak. Values of the ratio $Z(1\%)/Z(10\%)$ for different coastal areas and fjords are set out in Table 3.

In Fig. 5 the mean values of $K_d(310)$ are presented as a function of the mean salinities for the different coastal waters. Some results from adjacent oceanic areas have been added to illustrate the general tendency

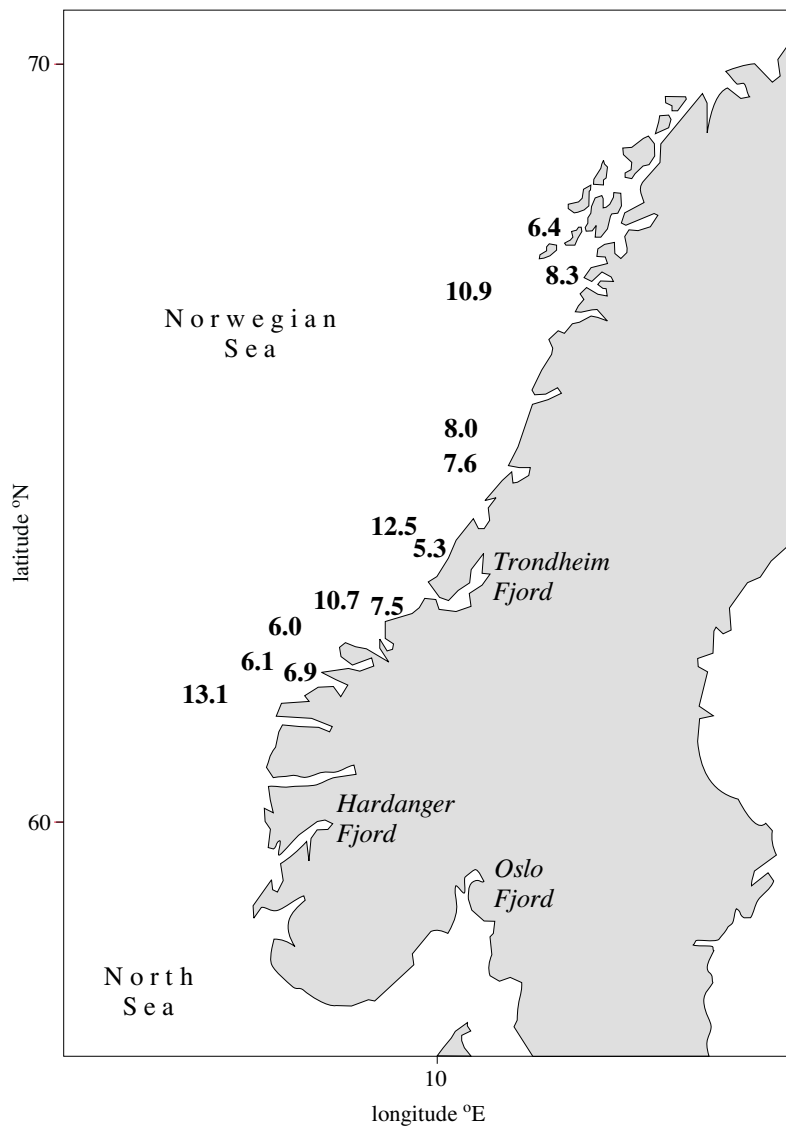


Fig. 4. $Z(380,10\%)$ [m] observed in the Norwegian Coastal Current during March–May 1967–71 (13 stations)

of this relationship. From the Baltic Sea only the single observation of UVB attenuation mentioned above has been found, with $K_d = 3.54 \text{ m}^{-1}$ and salinity = 7.6. This is represented by the small black circle in Fig. 5. However, based on the previously mentioned value of $a_y(380)$ for the core of Baltic Sea water, $K_d(380) \approx 1.2 \text{ m}^{-1}$ may be estimated from eq. (3) by assuming $a(380) \approx a_y(380) = 0.96 \text{ m}^{-1}$, $\mu_d \approx 0.80$, and $R \approx 0$. Provided

Table 1. Statistical properties of salinity and $Z(310,10\%)$ for the investigated areas

Area or water mass	Period	Salinity				$Z(310,10\%)$ [m]				Number of stations
		mean	min	max	SD	mean	min	max	SD	
Baltic-Danish c. w.	August–November 1976–77	8	–	–	–	1.3	0.7	2.5	1.0	3
Kattegat	May 1979	16.5	15.4	18.0	1.1	0.9	0.8	0.9	0.1	48
Oslo Fjord	February 2000	22.0	9.3	29.8	9.8	0.8	0.3	1.2	0.4	5
Skagerrak	March–April 1979	26.6	23.4	34.3	2.7	2.3	1.6	5.0	0.8	30
German Bight	August–September 1979	29.1	25.5	32.1	1.7	0.8	0.3	4.3	0.4	45
German Bight	June 1981	30.0	29.4	30.4	0.3	2.0	0.8	3.4	0.9	13
Norwegian Coast. Current ^a	March–May 1967–71	34.1	33.1	34.7	0.6	3.8	2.0	8.9	1.8	13
West Iceland c. w. ^a	August 1973	34.8	34.7	34.9	–	5.7	5.3	6.1	–	2

^a $Z(310,10\%)$ is calculated by eq. (16). Abbreviations: min – minimum value, max – maximum value, c. w. – coastal waters, SD – standard deviation.

Table 2. Statistical properties of salinity and $Z(380, 10\%)$ for the investigated areas

Area or water mass	Period	Salinity				$Z(380, 10\%)$ [m]				Number of stations
		mean	min	max	SD	mean	min	max	SD	
Hardanger Fjord	July 1967	4.2	2.5	9.0	2.3	1.4	0.8	2.5	0.6	7
Bornholm-Gotland	May 1973	7.7	7.6	8.2	0.3	2.1	1.5	2.9	0.4	10
Danish c. w.	April 1976, May–June 1977	10.8	7.8	17.8	4.8	1.4	1.2	1.5	0.1	4
Inner Oslo Fjord	February–November 1967	22.2	18.3	29.7	3.9	0.9	0.4	1.5	0.3	16
Inner Oslo Fjord	February–November 1973	24.3	19.3	28.2	3.4	1.0	0.7	1.4	0.3	8
Hardanger Fjord	May 1972	24.8	17.2	30.5	5.7	3.6	1.8	6.8	2.2	4
Hardanger Fjord	January 1970	32.80	32.80	32.80	–	7.5	7.3	7.7	–	2
Norwegian Coast. Current	March–May 1967–71	34.1	33.1	34.9	0.6	8.4	5.0	13.0	2.7	13
West Iceland c. w.	August 1973	34.8	34.7	34.9	–	8.3	8.3	8.3	–	2

Abbreviations as in Table 1.

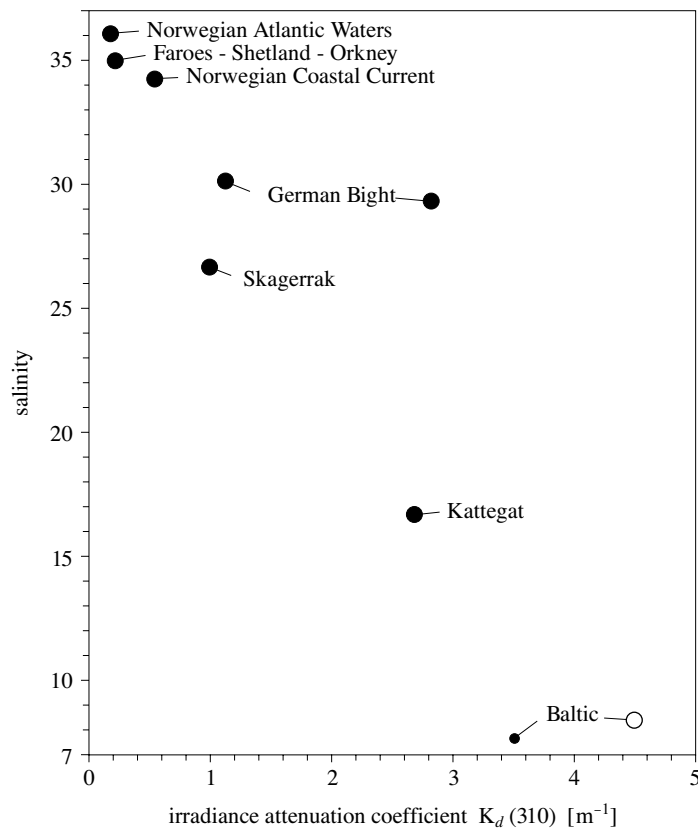


Fig. 5. Mean values of salinity and $K_d(310)$ for different open coastal waters and Atlantic waters. The small dot for the Baltic Sea represents one station, and the open circle is an estimated value

$K_d(\text{UV})$ is dominated by $K_y(\text{UV})$ and approximately follows eq. (8), $K_d(310)$ may be estimated from $K_d(380)$ by eq. (8) with $\gamma \approx 0.019 \text{ nm}^{-1}$ for the Baltic water (Kowalczyk & Kaczmarek 1996, Kowalczyk 1999). The estimated value of $K_d(310)$ then becomes 4.5 m^{-1} . This result is marked by the open circle in Fig. 5 for a salinity of 8.

5. Discussion

5.1. The investigation under review

5.1.1. Influence of solar elevation on $Z(10\%)$

The slope of the irradiance curves in the semilogarithmic diagram of Fig. 1 increases with increasing depth, implying that the vertical attenuation coefficient, defined by eq. (1), decreases with depth at this station. The

similarity in shape of these vertical profiles also confirms our earlier conclusion based on eq. (3), namely that the influence of solar elevation on the vertical attenuation is practically negligible in the UV spectral domain. This is an important property that greatly simplifies our comparison of different data sets of $Z(10\%)$.

5.1.2. Influence of a_y on $Z(10\%)$

According to our results (Table 1, Fig. 2), the mean value of $Z(310, 10\%)$ in the Skagerrak (2.3 m) is twice as high as in the Kattegat (0.9 m) and the German Bight (1.1 m for 1979 and 1981 together), although the salinity in the German Bight is the highest, implying a higher content of Atlantic water. However, it was pointed out in section 3 that the core waters of the German Bight can be characterised by a salinity of 31 and a rather high concentration of yellow substance, as expressed by $a_y(380) \approx 1.50 \text{ m}^{-1}$. This means that the Elbe, Weser and Ems rivers entering the German Bight, and the Rhine further to the west, must be extremely rich in yellow substance. If the water of the German Bight were a mixture of Atlantic water with a salinity of 35 and practically no absorption, and river water with salinity 0 and absorption coefficient $a_{y, \text{river}}(380)$, the latter coefficient should be a factor $35/(35-31) = 8.75$ times greater than for the German Bight, resulting in $a_{y, \text{river}}(380) \approx 13 \text{ m}^{-1}$. The value $a_y(387) = 9.2 \text{ m}^{-1}$ given by Kalle (1961) for the Lower Elbe is of the same order of magnitude. Doerffer (1979) presented a graph for the same location, where $a_y(380) = 6.1 \text{ m}^{-1}$. Warnock et al. (1999) extrapolated their absorption coefficients from the Southern Bight of the North Sea to zero salinity and found $a_y(387) = 3.29-5.38 \text{ m}^{-1}$. It should be noted that the particle content of the waters in the German Bight also may contribute significantly to K_d , although yellow substance in general is the dominant factor in the UV spectrum. Large differences occur within these areas. The average penetration depth $Z(310, 10\%)$ of the northern part of the German Bight, the Danish Wadden Sea, is represented by the number 2 in Fig. 2, which is 2–4 times higher than the numbers for the areas closer to the great German rivers. There are, however, coastal areas in the world where riverine particles dominate the UV attenuation. An example is the Yellow Sea, where $K_d(310) = 31.8 - 37.3 \text{ m}^{-1}$, of which particles are responsible for 93% (Højerslev 1988).

For comparison with the riverine values of a_y above it is interesting that Dera (1992) observed $a_y(350) = 15 \text{ m}^{-1}$ in the Vistula estuary of the Baltic Sea, probably corresponding to $a_y(380) \approx 8-9 \text{ m}^{-1}$. Ferrari et al. (1996) found values of $a_y(355)$ in the Vistula and nearby river mouths within the range 2–13 m^{-1} ($a_y(380) \approx 1-8 \text{ m}^{-1}$). Kowalczyk (1999) reports $a_y(400) = 14 \text{ m}^{-1}$ ($a_y(380) \approx 20 \text{ m}^{-1}$) as an extreme, unrepresentative value

for the mouth of the river Vistula and gives $a_y(400) = 0.25-3.33 \text{ m}^{-1}$ ($a_y(380) \approx 0.4-5 \text{ m}^{-1}$) as a statistically more reliable range for Southern Baltic bay water. In the Glomma estuary of the Oslo Fjord Sørensen has observed the range $a_y(380) = 2.3-9.8 \text{ m}^{-1}$ for salinities < 10 (Evenset et al. 1999).

The penetration depths $Z(310, 10\%)$ in Fig. 3 were obtained from $K_d(310)$ calculated from observed values of $K_d(380)$ and $K_d(465)$ by means of eq. (16). The model leading to eq. (16) can also produce estimates of the ratio $K_y(310)/K_d(310)$, resulting in $K_y(310)$ constituting $60 \pm 20\%$ of $K_d(310)$ in the Norwegian Coastal Current. Unfortunately, very few simultaneous measurements of K_d and a_y have been taken in the investigated areas. It is otherwise a common experience that field measurements of K_d and laboratory measurements of a_y are difficult to compare in coastal waters due to patchiness and vertical layering.

5.1.3. Relation between salinity and optical properties

The greatest UVB penetration depth for all oceans was observed in July 1988 in the Gulf of Mexico with the value $Z(310, 10\%) = 33.7 \text{ m}$ (Anon. 1989). The maximum value of $Z(380, 10\%)$ was observed in the same area but closer to the coast in April 1982 (Højerslev 1985), with a value around 34 m. The corresponding maxima in the Norwegian Current entering the Norwegian Sea are 17–18 m and 24–25 m (Højerslev & Aas 1991, Aas et al. 2001). The yellow substance content of this current is practically zero (Højerslev 1982), and its penetration depths are of interest because the upper limit of $Z(10\%)$ in the coastal waters will be determined by the optical properties of the oceanic waters mixing into the area and by the mixing rate. The maxima of the Norwegian Coastal Current, 9 and 13 m (Tables 1–2), are thus only about half of the corresponding values in the adjacent Atlantic waters. Figs. 3–4 show that the penetration depth increases with increasing distance from the coast. Increasing distance usually means increasing salinity and increasing content of Atlantic waters.

In Fig. 5 the vertical attenuation coefficient K_d is applied rather than the penetration depth $Z(10\%)$, because K_d is proportional to the absorption coefficient a (eq. 3), and after mixing different water types their absorption coefficients and salinities will mix in the same proportions. The figure illustrates the general tendency of coastal waters for K_d to decrease with increasing salinity. The points, however, do not form a straight line, indicating that there are several water types or riverine yellow substance inputs involved. Fig. 5 demonstrates clearly the anomalous influence of the river run-off to the German Bight.

5.1.4. $Z(10\%)$ in fjords

In the Oslo Fjord $Z(310, 10\%)$ typically varies in the range 0.1–1.0 m, where the smallest value represents the estuary of the river Glomma during the spring flood. In wintertime the yellow substance and particle content of the estuary is less, as can be seen from Table 1. Table 2 demonstrates that in the Inner Oslo Fjord at 380 nm the 10%-depth can change by a factor of 2–4 through the year, but the changes are unrelated to season. In the Hardanger Fjord, on the other hand, the change represents a factor of 10 and is clearly seasonal.

Unfortunately, we have no simultaneous measurements of UVB and UVA irradiance in the two different fjords, but we can obtain some idea of their spectral differences from the linear correlations between $Z(380, 10\%)$ and $Z(465, 10\%)$. For the Inner Oslo Fjord the analysis produces

$$Z(380, 10\%) = 0.42 \text{ m} + 0.19 Z(465, 10\%), \quad (28)$$

where $Z(465, 10\%)$ is in the range 1.1–4.9 m, while in the Hardanger Fjord the result becomes

$$Z(380, 10\%) = 0.58 \text{ m} + 0.28 Z(465, 10\%) \quad (29)$$

with $Z(465, 10\%)$ in the range 2.0–31.8 m. For all seasons the ratio $Z(380, 10\%)/Z(465, 10\%)$ will then be greater in the Hardanger Fjord than in the Oslo Fjord, due to the smaller content of yellow substance.

5.1.5. The ratio $Z(1\%)/Z(10\%)$

Most observations of $Z(1\%)/Z(10\%)$ lie in the range 2.0–2.2, although it is not unusual for values < 2.0 to occur, as can be seen from Table 3. According to our data set the strongest layering and the highest value of the ratio appear in the Kattegat in May 1979, and this feature can also be seen in Fig. 1.

5.2. Other authors

Measurements of UV irradiance in North European coastal waters taken by other authors cover the period from 1942 to 1999. Two early vertical profiles of assumed UVA irradiance from the English Channel, recorded by Atkins & Poole (1933), were obtained with a sensor and filter combination where the bandwidth may have been more than 100 nm. It can then easily be demonstrated that the main contribution to their signals must have come from the visible part of the spectrum. Later profiles from 1936 were attributed to the wavelength 400 nm by Poole & Atkins themselves (1937), while Johnson & Kullenberg (1946) quoted the same results with 375 nm as the representative wavelength. Due to these uncertainties the measurements from the English Channel have been rejected in our review.

Table 3. Ratio of the penetration depths $Z(1\%)$ and $Z(10\%)$

Area	Period	Wavelength [m]	$Z(1\%)/Z(10\%)$				Number of stations
			mean	min	max	SD	
Skagerrak	March–April 1979	310	2.16	1.62	2.94	0.24	30
Kattegat	May 1979	310	2.83	2.78	2.88	–	48
German Bight	August–September 1979	310	2.0	2.0	2.0	–	45
German Bight	June 1981	310	2.22	1.80	2.56	0.19	13
Inner Oslo Fjord	February–November 1967 and 1973	380	2.03	1.60	2.66	0.22	24
Norwegian Coast. Current	March–May 1967–71	380	2.05	1.72	2.47	0.18	13
Hardanger Fjord	July 1967	380	2.15	1.90	2.38	0.21	4
Hardanger Fjord	January 1970	380	2.18	2.17	2.19	–	2
Bornholm-Gotland	May 1973	380	1.93	1.67	2.33	0.22	9

Abbreviations as in Table 1.

Table 4. Values of $Z(310, 10\%)$ from other investigations

Area or water mass	Period	$Z(310, 10\%)$ [m]				Method	Number of stations	References
		mean	min	max	SD			
Gullmar Fjord	March–August 1944–45	0.44	0.08	1.02	0.27	T per dm	12	Johnson (1946)
Icelandic c. w.	1975–76 ^a	5.7	1.7	10.4	2.1	K_d	23	Calkins & Thordardottir (1982)
Norw. Coast. Curr.	April 1993 ^b	3.8	2.6	5.5	1.1	eq. (18)	5	Aas et al. (2001)
Baltic lagoons	May–August 1993	0.3	0.2	0.4	–	E_d	2	Piazena & Häder (1994)
Is Fjord	August 1993	3.8	0.9	4.8	1.4	E_d	6	Aas et al. (2001)
Inner Oslo Fjord	September 1994–May 1995	0.54	0.31	0.72	0.13	E_d	9	Aarseth (1997)
Trondheim Fjord	April 1995–December 1999	0.66	0.25	1.4	0.3	K_d	24	Kjeldstad (pers. comm.)
Kongs Fjord	June–July 1997 ^c	4.7	3.1	6.1	1.0	K_d 0–6 m	24	Hanelt et al. (2001)
Kongs Fjord	July–August 1998	3.6	3.1	4.5	0.4	K_d 0–6 m	17	Hanelt et al. (2001)

^aSecchi disc depth = 5–15 m, ^bSalinity = 34.0–34.9, ^cSalinity = 23.4–34.5. Abbreviations as in Table 1.

Table 5. Values of $Z(380, 10\%)$ from other investigations

Area or water mass	Period	$Z(380, 10\%)$ [m]				Method	Number of stations	References
		mean	min	max	SD			
Gullmar Fjord	August–October 1942 and March–August 1944–45	1.22	0.18	3.05	0.84	T per m	10	Johnson & Kullenberg (1946) and Johnson (1946)
Hardanger Fjord	July 1956	2.4	0.4	3.9	0.9	E_d	37	Aarthun (1958)
Norw. Coast. Curr.	April 1993 ^a	7.1	5.8	9.1	1.2	eq. (19)	5	Aas et al. (2001)
Baltic lagoons	May–August 1993	0.8	0.7	1.4	–	E_d 0–1.5 m	2	Piazena & Häder (1994)
Trondheim Fjord	April 1995–December 1999	1.5	0.31	3.8	0.6	K_d	35	Kjeldstad (pers. comm.)
Kongs Fjord	May–July 1998	3.1	2.1	4.5	1.3	K_d 0–5 m	3	Hanelt et al. (2001)

^aSalinity = 34.0–34.9. Abbreviations as in Table 1.

Very few of the authors present their observed UV attenuation as vertical profiles of irradiance or as tables for E_d at different depths. Unfortunately, quantities such as the vertical attenuation coefficient K_d or the transmittance T per m (alternatively per dm) will depend on the depth interval they are based on. If the vertical water column is layered, and if the applied depth interval is significantly different from the true value of $Z(10\%)$, errors will be introduced. In the Kattegat in May 1979 (Fig. 1) the depth $Z(310, 10\%)$ becomes overestimated by 70% if it is based on the mean value of K_d for the interval 0–6 m. The values presented in Tables 4–5 should then be regarded as tentative estimates.

The UVB transmittances (Table 4) observed by Johnson (1946) in the Gullmar Fjord on the West Coast of Sweden during 1944–45 were obtained with the special construction described in section 2.2. He also measured UVA irradiance in this fjord (Table 5) in 1942 and 1944–45 (Johnson 1946, Johnson & Kullenberg 1946) with a more conventional instrument equipped with Schott filters UG1 + BG12. As pointed out in section 2.2 this combination can be used to represent the irradiance at 380 nm down to the 1% level. The mean values of $Z(10\%)$ at 310 and 380 nm are among the smallest light penetration depths observed in coastal water.

Aarthun (1958) applied an instrument similar to the latter one with UG1 + BG12 in the Hardanger Fjord, but omitted the opal glass in order to increase the instrument's sensitivity. Nevertheless, his vertical profiles of UVA irradiance look reasonable, and the results of his complete series are presented in Table 5. An abridged extract of his thesis has been published (Aarthun 1961). A correlation analysis of the penetration depths at 380 and 465 nm produces

$$Z(380, 10\%) = 0.52 \text{ m} + 0.23 Z(465, 10\%), \quad (30)$$

which confirms the result of eqs. (28)–(29), namely that the UV-blue part of the irradiance spectrum is less steep in the Hardanger Fjord than in the Oslo Fjord.

Calkins & Thordardottir (1982) applied the Robertson meter north and west of Iceland during 1975–76, and 23 of their 30 stations were located within a distance of 100 km from the coast (Table 4). It has been demonstrated that in yellow substance-rich coastal water with $K_d(312) = 3.3 \text{ m}^{-1}$, the Robertson meter may underestimate the average value of $K_d(312)$ by 17% within the upper 3 m (Højerslev 1978). However, the maximum value of $K_d(\text{UVB})$ for the present coastal stations was 1.35 m^{-1} , and at 20 of the stations K_d was less than 0.6 m^{-1} . Their figures indicate that the UVB irradiance was measured down to about 8 m, and consequently we have neglected the error mentioned with regard to the statistical results presented in Table 4.

Extensive bio-optical measurements were made during the CARDEEP program in 1993 and 1994 where downward irradiance in the visible spectrum was recorded with the MER-1032 Reflectance Spectroradiometer from Biospherical Instruments. Parts of this material have been published by Dalløyken et al. (1994, 1995) and Aas et al. (2001). The values for $Z(310, 10\%)$ and $Z(380, 10\%)$ from the Norwegian Coastal Current presented in Tables 4–5 are estimates obtained by eqs. (18)–(19), based on observations at 410 and 465 nm. The results are very close to the values presented in Tables 1–2 for the same current.

Piazena & Häder (1994) measured UV irradiance in two coastal lagoons of the Southern Baltic Sea. Their instruments were double monochromator spectroradiometers from Optronic Laboratories. The values of $Z(310, 10\%)$ and $Z(380, 10\%)$ in Tables 4–5, tentatively estimated from their figures, represent the smallest penetration depths in these tables.

The UVB irradiance in the Is Fjord at West Spitsbergen was recorded by Høkedal in 1993 with the Hundahl construction described in section 2.2. The same instrument was later applied by Aarseth (1997), who studied the reaction of copepods to UVB irradiance in the Inner Oslo Fjord from September 1994 to May 1995 (Table 4). His results lie within the range observed in February 2000 (Table 1).

More UV recordings in fjord water were made by Kjeldstad et al. (2000) in the Trondheim Fjord during 1995–99 at the position 63.29°N, 10.18°E, located at the most open and wide part of the fjord. The instrument was the four-channel radiometer GUV 500/510 from Biospherical Instruments. The observed range of $Z(380, 10\%)$ in the Trondheim Fjord (Table 5) is three times the corresponding range of the Inner Oslo Fjord (Table 2).

The final fjord measurements in Tables 4–5 were made in the Kongs Fjord at West Spitsbergen with a special UVB sensor for the range 280–320 nm (Bischof et al. 1998, Hanelt et al. 2001). It should be noted that the estimated depths of $Z(310, 10\%)$ are based on average values of $K_d(\text{UVB})$ for the depth range 0–6 m. Spectral irradiance in the UVA and visible range was determined with a spectroradiometer based on a cosine diffuser and a diode array.

6. Conclusions

In our investigation the range of $Z(310, 10\%)$ in open North European coastal waters, based on 154 stations, is 0.3–8.9 m. If we add the 28 stations reported by other authors, the maximum depth increases to 10.4 m. Only 29 measurements of $Z(380, 10\%)$ were taken by ourselves in open coastal waters, and we have found 5 recordings made by other authors. The resulting

range is 1.2–13.0 m. At both wavelengths $Z(10\%)$ varies by at least one order of magnitude. Mixing with oceanic waters can increase the penetration depths to more than 10 m.

In fjord waters 5 observations of $Z(310, 10\%)$ were made by ourselves and 94 by other authors; the combined range is from 0.08 to 6.1 m. $Z(380, 10\%)$ was measured at 37 stations in fjord water by ourselves and at 87 stations by other authors. The total range is 0.18–7.7 m. As expected, the relative variation is greater in fjords and estuaries than in coastal waters, because river run-off can reduce the penetration depths to only a few centimetres.

Most of the penetration depths discussed here represent summer situations, usually based on single expeditions in one or two years. We have no quantified information about the seasonal variation in the open coastal waters. We have seen that in fjords and estuaries seasonal changes in river run-off may create significant changes in the optical properties as, for example, in the Sogne Fjord, where the Secchi disc depth was reported to increase from 1 m in summer to 26 m in winter.

Altogether 439 measurements of UV irradiance in North European coastal waters have been discussed, half of which originate from other authors. This data set can be considered as a beginning of a UV mapping of these waters. Although in some coastal areas a lot of optical measurements have been made over the years, recordings of UV irradiance are still lacking. In many other areas most kinds of optical measurements are missing.

References

- Aarseth K. A., 1997, *Ultrafiolett stråling og det marine miljø. Betydningen av UV-B for utvalgte copepoder i laboratorieforsøk*, Thesis, Dept. Biol., Univ. Oslo.
- Aarthun K. E., 1958, *Submarine lysforhold i Hardangerfjorden*, Thesis, Dept. Geography, Univ. Oslo.
- Aarthun K. E., 1961, *The natural history of the Hardangerfjord. 2. Submarine daylight in a glacier-fed Norwegian fjord*, Sarsia, 1, 7–20.
- Aas E., 1969, *On submarine irradiance measurements*, Rep. Dept. Phys. Oceanogr., Univ. Copenhagen, 6.
- Aas E., 1971, *The natural history of the Hardangerfjord. 9. Irradiance in Hardangerfjorden 1967*, Sarsia, 46, 59–78.
- Aas E., 1976, *The vertical attenuation coefficient of submarine irradiance*, Rep. Dept. Geophys., Univ. Oslo, 19.
- Aas E., Høkedal J., 1996, *Penetration of ultraviolet B, blue and quanta irradiance into Svalbard waters*, Polar Res., 15, 127–138.
- Aas E., Høkedal J., 1999, *Reflection of spectral sky irradiance on the surface of the sea and related properties*, Remote Sens. Environm., 70, 181–190.

- Aas E., Høkedal J., Højerslev N.K., Sandvik R., Sakshaug E., 2001, *Spectral properties and UV-attenuation in Arctic marine waters*, [in:] *UV-radiation and Arctic ecosystems*, D. O. Hessen (ed.), Springer-Verlag, Heidelberg, submitted.
- Anon., 1989, *Gulf of Mexico. Physical oceanography program. Final report: year 5*, U.S. Dept. Interior, Mineral Management Service, Gulf of Mexico OCS Regional Office, New Orleans. OCS Study MMS 89-0068.
- Atkins W.R.G., Poole H.H., 1933, *The photo-electric measurements of the penetration of light of various wave-lengths into the sea and the physiological bearing of the results*, Phil. Trans. R. Soc., 222 (B), 129-164.
- Aure J., Sætre R., 1981, *Wind effects on the Skagerrak outflow*, [in:] *The Norwegian Coastal Current*, R. Sætre & M. Mork (eds.), Proc. Univ. Bergen, 263-293.
- Austin R. W., Petzold T. J., 1984, *Spectral dependence of the diffuse attenuation coefficient of light in ocean water*, Ocean Optics VII, Proc. SPIE - Int. Soc. Opt. Eng., 489, 168-178.
- Austin R. W., Petzold T. J., 1990, *Spectral dependence of the diffuse attenuation coefficient of light in ocean waters: a re-examination using new data*, Ocean Optics X, Proc. SPIE - Int. Soc. Opt. Eng., 1302, 79-93.
- Bischof K., Hanelt D., Tüg H., Karsten U., Brouwer P.E.M., Wiencke C., 1998, *Acclimation of brown algal photosynthesis to ultraviolet radiation in Arctic coastal waters (Spitsbergen, Norway)*, Polar Biol., 20, 388-395.
- Calkins J. (ed.), 1982, *The role of solar ultraviolet radiation in marine ecosystems*, Plenum Press, New York, 724 pp.
- Calkins J., Thordardottir T., 1982, *Penetration of solar UV-B into waters off Iceland*, [in:] *The role of solar ultraviolet radiation in marine ecosystems*, J. Calkins (ed.), Plenum Press, New York, 309-319.
- Dalløkken R., Sandvik R., Sakshaug E., 1994, *Variations in bio-optical properties in the Greenland/Iceland/Norwegian seas*, Ocean Optics XII, Proc. SPIE - Int. Soc. Opt. Eng., 2258, 266-276.
- Dalløkken R., Sandvik R., Sakshaug E., 1995, *Seasonal variations in the Greenland Sea: effect of phytoplankton light absorptions*, [in:] *Ecology of fjords and coastal waters*, H. R. Skjoldal, C. Hopkins, K. E. Erikstad & H. P. Leinaas (eds.), Elsevier, Amsterdam, 33-43.
- Dera J., 1992, *Marine physics*, PWN, Warszawa, Elsevier, Amsterdam, 516 pp.
- Doerffer R., 1979, *Untersuchungen über die Verteilung oberflächennaher Substanzen im Elbe-Aestuar mit Hilfe von Fernmessverfahren*, Arch. Hydrobiol. Suppl., 43, 119-224.
- Dooley H. D., Furnes G. K., 1981, *Influence of the wind field on the transport of the Northern North Sea*, [in:] *The Norwegian Coastal Current*, R. Sætre & M. Mork (eds.), Proc. Univ. Bergen, 57-71.

- Evenset A., Dahle S., Loring D., Skei J., Sørensen K., Cochrane S., Carrol J., Forsberg C. F., Fredriksen K.-R., 1999, KAREX '94: an environmental survey of the Kara Sea and the estuaries of Ob and Yenisey, Akvaplan-niva Tromsø, Rep. APN 414.96.1006.
- Fahey D. W., 1995, *Polar ozone*, [in:] *Scientific assessment of ozone depletion: 1994*, C. A. Ennis (ed.), WMO/UNEP, Global Ozone Res. Monitor. Proj., Rep. No. 37, Pp. 3.1–3.52.
- Farman J. C., Gardiner B. G., 1987, *Ozone depletion over Antarctica*, *Nature*, 329, p. 574.
- Farman J. C., Gardiner B. G., Shanklin J. D., 1985, *Large losses of ozone in Antarctica reveal seasonal ClO_x/NO_x interaction*, *Nature*, 315, 207–210.
- Ferrari G. M., Dowell M. D., Grossi S., Targa C., 1996, *Relationship between the optical properties of chromophoric dissolved organic matter and total concentration of dissolved organic carbon in the southern Baltic Sea region*, *Mar. Chem.*, 55, 299–316.
- Furnes G. K., Sælen O. H., 1977, *Currents and hydrography in the Norwegian Coastal Current off Utsira during JONSDAP'76*, Norw. Coastal Current Proj., Rep. No. 2, Univ. Bergen.
- Gershun A., 1939, *The light field*, *J. Math. Phys.*, 18, 51–151.
- Gieskes W. W. C., Kraay G. W., 1990, *Transmission of ultraviolet light in the Weddel Sea: report of the first measurements made in the Antarctic*, *Biomass Newsletter*, 12, 12–14.
- Hanelt D., Tüg H., Bischof K., Gross C., Lippert H., Sawall T., Karsten U., Wiencke C., 2001, *Light regime in an Arctic fjord: a study related to stratospheric ozone depletion as a basis for determination of UV effects on algal growth*, *Mar. Biol.*, 138, 649–658.
- Helbling E. W., Holm-Hansen O., Villafañe V., 1994, *Effects of ultraviolet radiation on Antarctic marine phytoplankton photosynthesis with particular attention to the influence of mixing*, [in:] *Ultraviolet radiation in Antarctica: measurements and biological effects*, C. S. Weiler & P. A. Penhale (eds.), Antarctic Res. Ser. (Am. Geophys. Union, Washington, DC), 62, 207–227.
- Høgerslev N. K., 1973, *Inherent and apparent optical properties of the Western Mediterranean and the Hardangerfjord*, Rep. Dept. Phys. Oceanogr., Univ. Copenhagen, 21.
- Høgerslev N. K., 1974, *Inherent and apparent optical properties of the Baltic*, Rep. Dept. Phys. Oceanogr., Univ. Copenhagen, 23.
- Høgerslev N. K., 1978, *Solar middle ultraviolet (UV-B) measurement in coastal waters rich in yellow substance*, *Limnol. Oceanogr.*, 23, 1076–1079.
- Høgerslev N. K., 1982, *Yellow substance in the sea*, [in:] *The role of solar ultraviolet radiation in marine ecosystems*, J. Calkins (ed.), Plenum Press, New York, 263–281.
- Høgerslev N. K., 1985, *Bio-optical measurements in the Southwest Florida Shelf ecosystem*, *J. Cons. int. Explor. Mer.*, 42, 65–82.

- Højerslev N. K., 1988, *Natural occurrences and optical effects of Gelbstoff*, Rep. Dept. Geophys., Univ. Copenhagen, 50.
- Højerslev N. K., Aas E., 1991, *A relationship for the penetration of ultraviolet B radiation into the Norwegian Sea*, J. Geophys. Res., 96, 17003–05.
- Højerslev N. K., Aas E., 2001, *Spectral light absorption by yellow substance in the Kattegat-Skagerrak area*, Oceanologia, 43 (1), 39–60.
- Højerslev N. K., Holt N., Aarup T., 1996, *Optical measurements in the North Sea-Baltic Sea transition zone. I. On the origin of deep water in the Kattegat*, Cont. Shelf Res., 16, 1329–1342.
- Højerslev N. K., Lundgren B., 1977, *Inherent and apparent optical properties of Icelandic waters 'Bjarni Sæmundsson Overflow 73'*, Rep. Dept. Phys. Oceanogr., Univ. Copenhagen, 33.
- Høkedal J., Aas E., 1994, *Calibration of two single-channel instruments for UV-B and blue irradiance*, Rep. Dept. Geophys., Univ. Oslo, 88.
- Jerlov N. G., 1951, *Optical studies of ocean water*, Rep. Swedish Deep-Sea Exped., 3, 1–59.
- Jerlov N. G., 1976, *Marine optics*, Elsevier, Amsterdam, 231 pp.
- Johnson (Jerlov) N. G., 1946, *On anti-rachitic ultra-violet radiation in the sea*, Medd. Oceanogr. Inst. Göteborg, ser. B, Bnd. 3, 11.
- Johnson (Jerlov) N. G., Kullenberg B., 1946, *On radiant energy measurements in the sea*, Svenska Hydrografisk-biologiska kommissionens skrifter, 3. series, 1 (1).
- Kalle K., 1961, *What do we know about the 'Gelbstoff'?*, [in:] *Symposium on radiant energy in the sea, Helsinki, 4–5 August 1960*, N. G. Jerlov (ed.), UGGI, Monographie, 10, 59–62.
- Kjeldstad B., Olsen Y., Børsheim Y., Stokke K., Storsveen G., Sakshaug E., 2000, *Seasonal UV penetration variability in a Norwegian fjord system; sources and interpretations*, [in:] *Ocean Optics XV, Monaco, October 16–20 2000*, CD-ROM.
- Kowalczyk P., Kaczmarek S., 1996, *Analysis of temporal and spatial variability of 'yellow substance' absorption in the southern Baltic*, Oceanologia, 38 (1), 3–32.
- Kowalczyk P., 1999, *Seasonal variability of yellow substance absorption in the surface layer of the Baltic Sea*, J. Geophys. Res., 104, 30047–30058.
- Kuhn P., Browman H., McArthur B., StPierre J. F., 1999, *Penetration of ultraviolet radiation in the waters of the estuary and Gulf of St. Lawrence*, Limnol. Oceanogr., 44, 710–716.
- Laurion I., Vincent W. F., Lean D. R. S., 1997, *Underwater ultraviolet radiation: development of spectral models for northern high latitude lakes*, Photochem. Photobiol., 65, 107–114.
- Markager S., Vincent W. F., 2000, *Spectral light attenuation and the absorption of UV and blue light in natural waters*, Limnol. Oceanogr., 45, 642–650.
- Midttun L., 1971, *Long term observation series of surface temperature and salinity in Norwegian coastal waters*, ICES, C. M. 1971/C:25.

- Montecino V., Pizarro G., 1995, *Phytoplankton acclimation and spectral penetration of UV irradiance off the central Chilean coast*, Mar. Ecol. Progr. Ser., 121, 261–269.
- Morris D.P., Zagarese H., Williamson C.E., Balseiro E.G., Hargreaves B.R., Modenutti B., Moeller R., Queimalinos C., 1995, *The attenuation of solar UV radiation in lakes and the role of dissolved organic carbon*, Limnol. Oceanogr., 40, 1381–1391.
- Piazena H., Häder D.-P., 1994, *Penetration of solar UV irradiation in coastal lagoons of the southern Baltic Sea and its effect on phytoplankton communities*, Photochem. Photobiol., 60, 463–469.
- Poole H.H., Atkins W.R.G., 1937, *The penetration into the sea of light of various wave-lengths as measured by emission or rectifier photo-electric cells*, Proc. R. Soc. London, ser. B, 123, 151–165.
- Rustad D., 1978, *Hydrographical observations from Sognefjorden*, Univ. Trondheim, R. Norw. Soc. Sci. Lett., The Museum, Gunneria, 30.
- Smith R.C., Prézelin B.B., Baker K.S., Bidigare R.R., Boucher N.P., Coley T., Karentz D., MacIntyre S., Matlick H.A., Menzies D., Ondrusek M., Wan Z., Waters K.J., 1992, *Ozone depletion: ultraviolet radiation and phytoplankton biology in Antarctic waters*, Science, 255, 952–959.
- Stambler N., Lovengreen C., Tilzer M.M., 1997, *The underwater light field in the Bellingshausen and Amundsen Seas (Antarctica)*, Hydrobiol., 344, 41–56.
- Sælen O.H., 1967, *Some features of the hydrography of Norwegian fjords*, [in:] Estuaries, G.H. Lauff (ed.), Am. Ass. Adv. Sci., Publ., 83, 63–70.
- Tollan A., 1976, *River runoff in Norway*, [in:] *Fresh water on the sea*, S. Skreslet, R. Leinebø, J.B.L. Matthews & E. Sakshaug (eds.), Proc. Symp. April 1974, Ass. Norw. Oceanogr., Oslo, 11–13.
- Warnock R.E., Gieskes W.W.C., van Laar S., 1999, *Regional and seasonal differences in light absorption by yellow substance in the Southern Bight of the North Sea*, J. Sea Res., 42, 169–178.
- Wyrki K., 1954, *Schwankungen im Wasserhaushalt der Ostsee*, Dt. Hydrogr. Z., 7, 91–129.